

Nonlinear Compression Behavior of Warp-Knitted Spacer Fabric: Effect of Sandwich Structure

Xiaonan Hou¹, Hong Hu¹, Yanping Liu¹ and Vadim Silberschmidt²

Abstract: Compressibility of warp-knitted spacer fabrics is one of their important mechanical properties with regard to many special applications such as body protection, cushion and mattresses. Due to specific structural features of the fabric and a non-linear mechanical behavior of monofilaments, the compression properties of this kind of fabrics are very complicated. Although several studies have been performed to investigate their compression behavior, its mechanism has not well been understood yet. This work is concerned with a study of compression mechanism of a selected warp-knitted spacer fabric with a given sandwich structure. Both experimental and numerical methods are used to study the effect of the material's structure on the overall compression mechanism. Compression tests are conducted to obtain force-displacement relationships of the fabric. A micro-computed tomography system is used to analyze specimens under different levels of compression displacement to investigate the change in material's structure during the compression process. At the same time, finite element models are developed separately to simulate the initial geometric structure and the compression behavior of the fabric. Three finite element models based on beam elements are firstly developed to simulate the effect of manufacturing process on shapes of monofilaments within the fabric and to determine their morphologies, which are used to assemble a geometry part of the finite element model of the overall fabric. Then the finite-element model is developed using beam and shell elements to describe the compression behavior of the fabric by introducing the effect of its complex microstructure and real non-linear mechanical properties of the monofilaments. A comparison of the obtained experimental and CT data, and results of simulation is carried out, demonstrating a good agreement. With this study, a compression mechanism of the warp-knitted spacer fabric can be better understood.

Keywords: Warp-knitted spacer fabric; Finite element analysis; Compression mechanism

¹ The Hong Kong Polytechnic University, Hong Kong

² Loughborough University, Loughborough, UK

1 Introduction

Spacer fabrics are three-dimensional sandwich structures consisting of two separate outer fabric layers, which are joined together with a layer of monofilaments (Figure 1). They can be manufactured by using different technologies (warp knitting, weft knitting and weaving) and materials (multifilament and monofilament) to achieve specific required mechanical properties for a number of practical applications, including body protection [Skock-Hartmann et al. (2009)], cushion materials [Ye, Hu & Feng (2008)], car seats [Ye, Hu & Araujo (2007)] and building construction [Arbakan, Roye (2009)]. One of the most important mechanical properties is the compression resistance which is linked with the specific sandwich structure of spacer fabrics. Some efforts have been done to experimentally investigate the compression behavior of such fabrics [Arbakan, Roye (2009); Yip, Ng (2008); Miao, Ge (2008); Liu, Hu (2011)]. However, the main limitation in experimental investigations is a lack of a suitable method for the simultaneous observation of the deformation of monofilaments within the fabric during the overall compression process, and thus it is hard to estimate the effect of material's microstructure on the effective mechanical properties of the fabric. Besides, it is expensive to prepare a large number of samples, which is essential to the experiments of fabrics. So, alternative ways have been sought, with numerical simulations being the main approach. Sheikhzadeh *et al.* firstly developed a numerical model to simulate the compression behavior of spacer fabrics based on the Van Wyk's compression theory [Wyk (1946)] by ignoring the geometric features of the fabric [Sheikhzadeh et al. (2010)]. As their model is based on a continuous structure, the mechanical properties of the overall fabric cannot be linked with the fabric's real microstructure. Therefore, models based on discontinuous microstructure are usually developed for engineering fabrics [Hou, Acar and Silberschmidt 2009; Hou, Acar and Silberschmidt (2011b); Hou, Acar & Silberschmidt (2011a)]. At present, the only finite element model developed for spacer fabrics with introducing the microstructure of the sample material is that of Vassiliadis *et al.* [Vassiliadis et al. (2009)]. However, the model only focused on a type of spacer fabric with a symmetric structure (i.e. the shape of its monofilaments is symmetric with regard to the horizontal axial, and each unit cell is symmetric with regard to the vertical axial. Besides, the outer layers of the model were discontinuous and no contact was included. Moreover, the model also assumed that the monofilaments are elastic. Therefore, that model cannot describe a generalized compression behavior of spacer fabrics, which is more complicated and combined with compression, shearing, bending, and contacts modes.

The present paper reports a work using both experimental and numerical methods to study the compression behavior of a warp-knitted spacer fabric by considering non-linear material properties of monofilaments, their shearing and bending, com-

pression of outer layers and contact between monofilaments and outer layers. It is expected that the compression mechanism of the spacer fabric can be better understood with the obtained results.

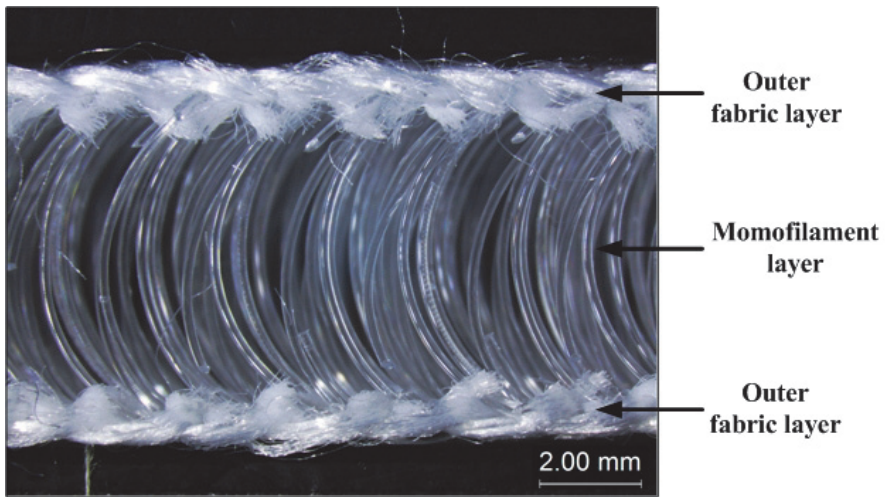
2 Warp-knitted spacer fabric: microstructure and compression behavior

The warp-knitted spacer fabric manufactured on a double-needle bar Raschel machine GE296 (RD6) of gauge E18 is used in this study; its microstructure is shown in Figure 1. The middle layer of the fabric consists of spacer yarns, which are formed with unsymmetrical curved polyester monofilaments of 0.2 mm in diameter and are connected together with outer layers (Figure 1a). The outer layers are knitted with multifilament (Figure 1b). The thickness of the fabric is 7.52 mm.

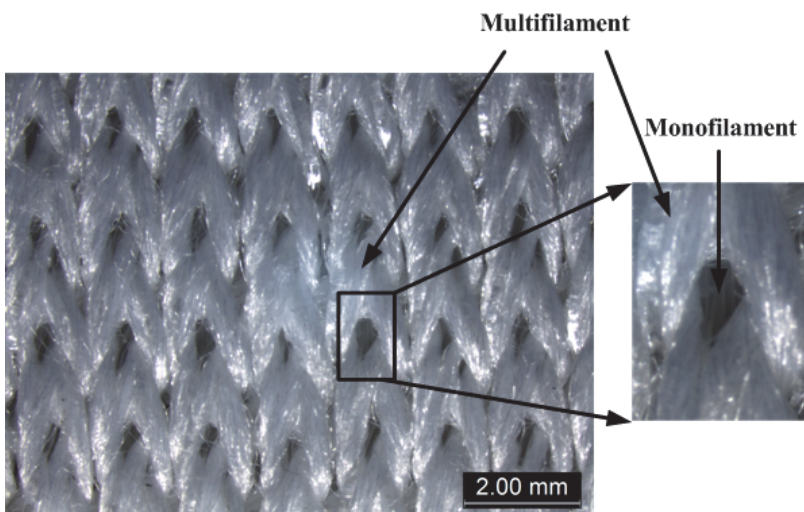
As a result of the special sandwich structure of the spacer fabric, the mechanical properties of the material are rather non-trivial, especially its compression property. Figure 2 shows a typical load-displacement relationship of the fabric under compression. The specimens were tested using the INSTRON 5566 machine. The areas of specimens are 100 mm × 100 mm. They were compressed with their bottom surface stuck to the fixed compression plate and a constant displacement rate was applied to another surface. The speed in the experiments was 12 mm/min.

In order to investigate the change of fabric structure during the compression process, a smaller specimen (20 mm × 20 mm) is scanned with a micro-CT system (Scanco/VivaCT 40). A specified jig is designed as shown in Figure 3. The specimen is compressed by compression stages to different displacement levels (0 mm, 1 mm, 2 mm, 3.3 mm), and the obtained slides are then re-constructed to built 3-D models (Figure 4).

Due to the non-symmetric and complex sandwich structure of the material, a highly nonlinear behavior was obtained in compression tests. To analyze the unique compression behavior of the fabric, the compression deformation is divided into four different stages (I, II, III and IV, see Figure 2) according to the changes in the slope of the curve. They are defined as initial stage (stage I), second stage (stage II), third stage (stage III) and final stage (stage IV). At the initial stage of the deformation, a lower slope is determined by the inherently loose microstructure of the fabric. As shown in Figure 5, the monofilaments are knitted within the outer layers, and voids can be found in the connection areas. Obviously, multifilaments around a monofilament do not contribute to its rotational constraint at the initial stage of the compression deformation. When the fabric is further compressed (second stage, shown in Figure 2), a stiffer mechanical performance is obtained. The phenomenon could be a result of the fastened microstructure of the fabric. The monofilaments rotate and deform, and the multifilaments start constraining them. According to the



(a)



(b)

Figure 1: Structure of spacer fabric: (a) side view of the material; (b) outer surface of outer layer

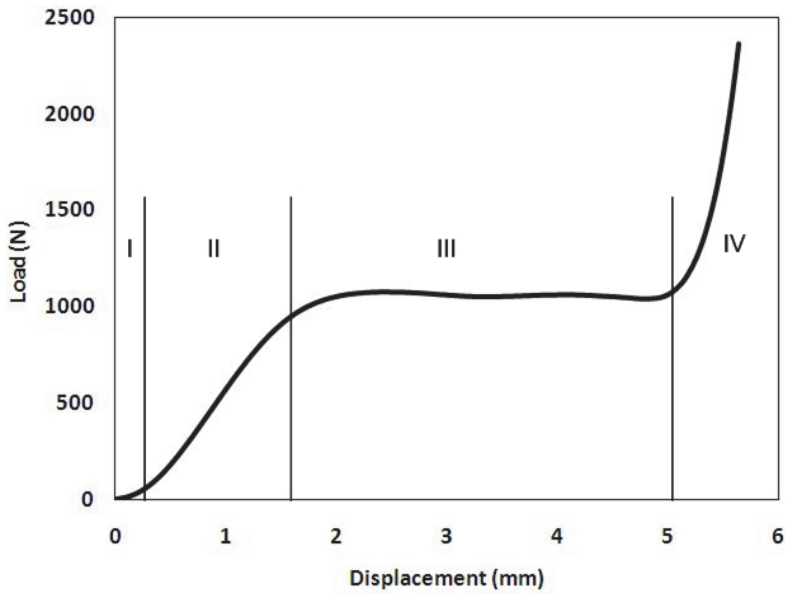


Figure 2: Typical compressive load-displacement relationship of spacer fabric

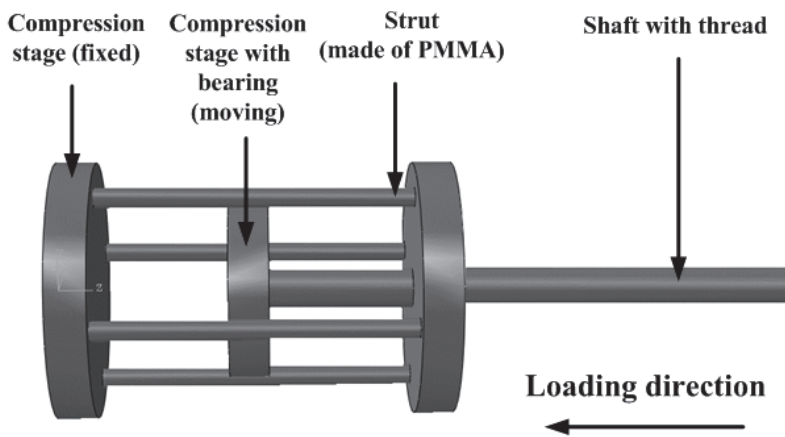


Figure 3: Compression jig designed for micro-CT scanning

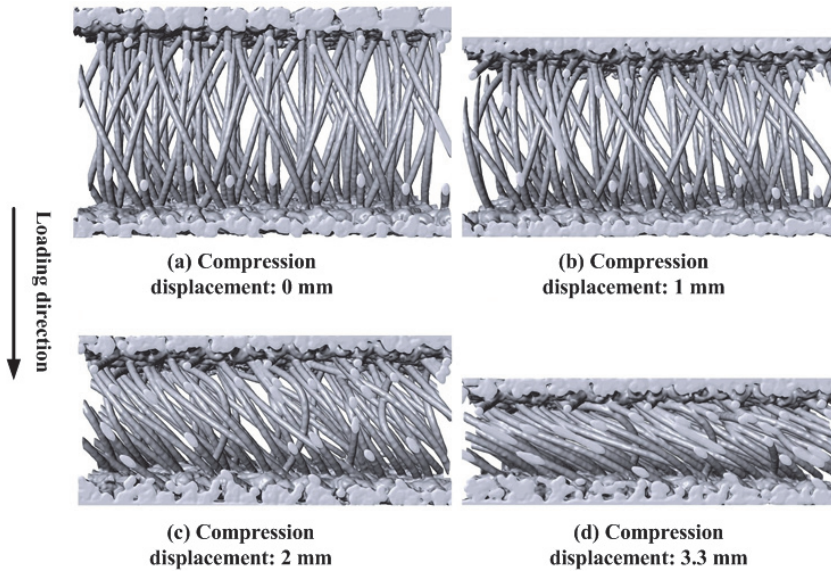


Figure 4: Results of micro-CT scan (un-deformed and deformed specimen models)

CT reconstructed model (Figure 4b), the overall structure starts to shear slightly in the plane of material's outer layers. The most important behavior of the spacer fabric is its third stage (shown in Figure 2). A nearly constant load is obtained, with the fabric being continuously compressed. This provides the material a good compression and impact resistance. However, the deformation mechanism of the fabric at this stage is very complicated and interesting; it is affected by the collapse, bending, shearing of the monofilaments and the change of the microstructure of the outer layers. At this stage, the inter-force between monofilaments and multifilament could be higher than the static inter-fiction, giving more freedom to the monofilaments. Hence, larger shear and collapse is observed (Figure 4c and 4d), and the reaction force stops rising. The final stage of compression shows a fast increase in the load, which is caused by swift densification of the entire fabric. At this stage, monofilaments within the fabric collapse and contact each other due to the constraint provided by the outer layers. Therefore, a really high stiffness is observed.

3 Finite element model of monofilament

Due to the complicated sandwich microstructure of the spacer fabric, it is hard to measure the morphologies and dimensions of the monofilaments in the middle

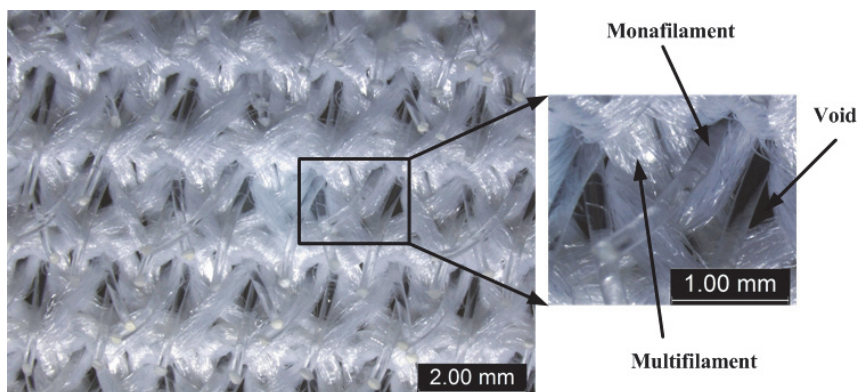


Figure 5: Microstructure of internal side of fabric's outer layer

layer experimentally. Therefore, the finite element method was used to simulate the manufacturing process and determine their shape and dimensions. According to the manufacturing mechanism of the knitting machine and the manufacturing parameters, a simplified scheme (Figure 6) was introduced into finite element simulations. There are three different shapes of monofilaments in the fabric: curve 1, curve 2 and curve 3. Their shapes and dimensions are determined by their initial positions and manufacturing process. Three FE models were developed to predict their shapes and dimensions individually. As shown in Figure 6, the straight monofilaments are compressed and buckled to curves in the simulations.

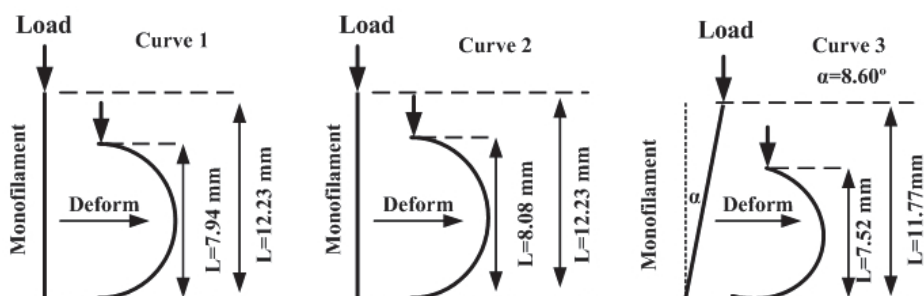


Figure 6: Scheme of FE models for monofilaments

The elasto-plastic property of monofilament was introduced into the FE models as shown Figure 7, based on the experimental data; the Poisson's ratio was 0.3.

The results of the FE models are shown as Figure 8. And these deformed parts are

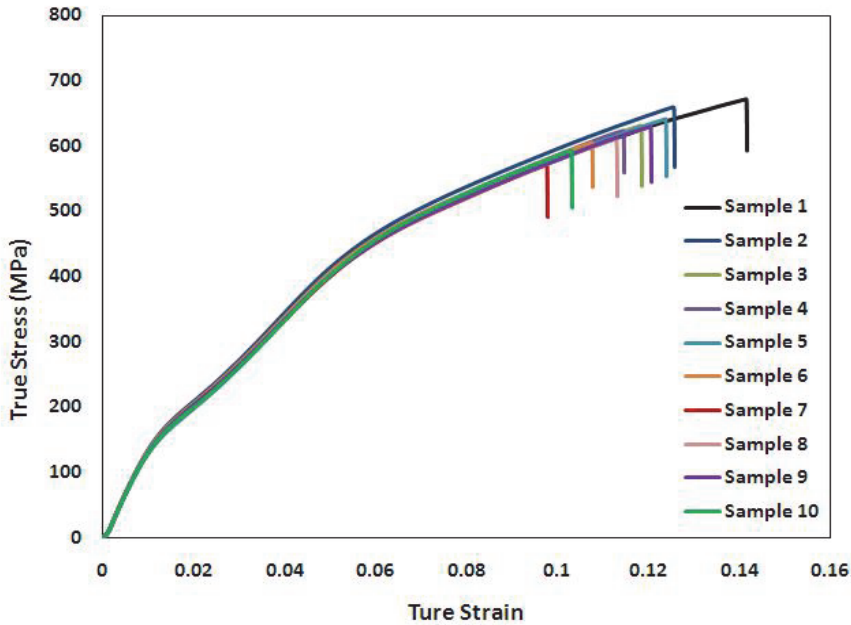


Figure 7: Stress – strain relationship of polyester monofilament within the spacer fabric

then introduced into the FE model to construct the geometric part of the overall fabric.

4 Finite element model of spacer fabric

To analyze the compression mechanism of the spacer fabric, a finite element model was developed. The results of numerical simulation, based on this model, are compared with the experimental data. The geometry of the spacer fabric is complicated, since it consists of a large number of monofilaments and multifilaments. Therefore, a representative unit, i.e. the smallest element including all the geometric features of the overall fabric, was determined to represent the overall fabric. It consists of two outer layers and a monofilament layer. The monofilament layer includes eight monofilaments with different shapes (Figure 9): two of curve 1, two of curve 2, and four of curve 3. They were meshed using beam elements B31 of ABAQUS and elasto-plastic properties of real monofilaments were used. The two outer layers were simplified as two planes (Figure 10a) simplifying their complicated microstructure; and they were meshed with shell elements S4R. Elastic

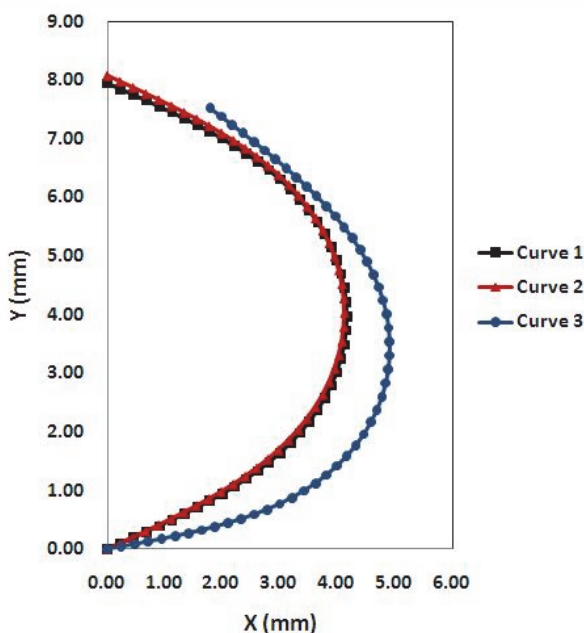


Figure 8: Shapes and dimensions of monofilaments within the spacer fabric

isotropic properties were defined for the outer layers: Young’s modulus: 13341.74 MPa, and Poisson’s ratio: 0.3.

The boundary conditions of the model are hard to define due to the fabric’s loose structure. Especially, the constraints between monofilaments and outer layers could change during the compression process. Therefore, the simulation was divided into two steps to apply different boundary conditions at different stages of deformation. The boundary conditions of the model were applied as follows: its bottom was fixed as “ENCASTRE” at all steps of the simulation. All the degrees of freedom of the nodes located at that boundary were constrained. Such boundary condition corresponds to fixture of the specimen in a compression plane in the real-life test. A uniform displacement in a negative y direction was applied to the upper outer layer of the model to simulate the static compression deformation. However, translations of the surface along x and z were not constrained. This allowed the outer layer to slide in x-z plane, as usually observed in the experiments. During step 1, the displacement was -0.2 mm. Then, the model was continuously compressed to -5.0 mm during step 2, i.e. the FE model was developed to describe the compression stages I, II and III. For compression stage IV, the deformation mechanism is obvious and hence not included in the present model.

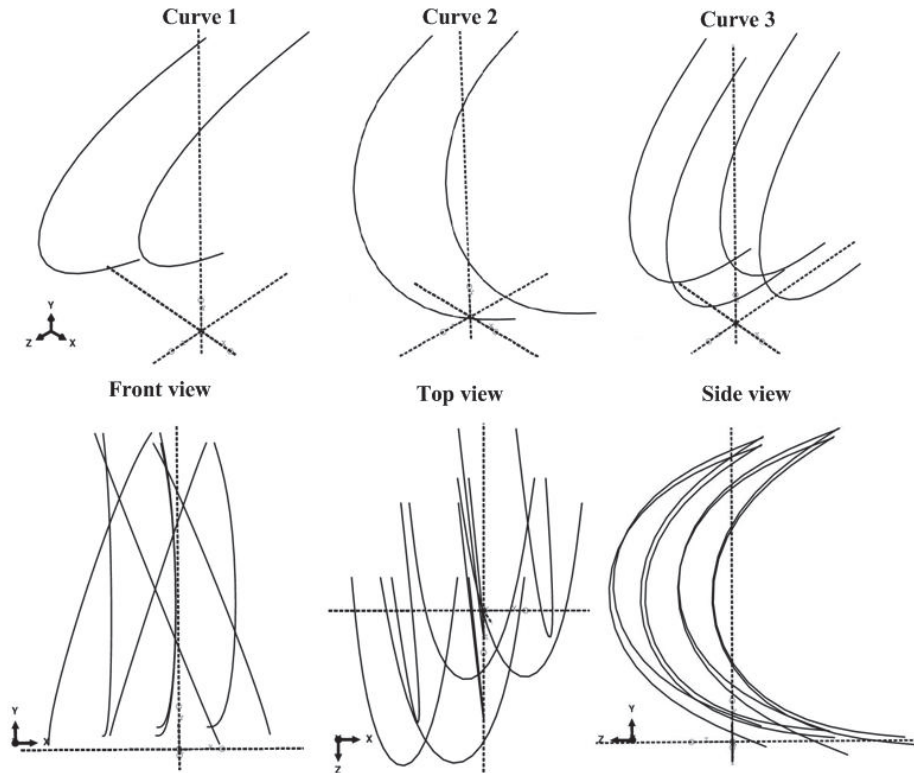


Figure 9: Geometry part of monofilament layer of unit cell in finite element model: upper row – constituent monofilaments; lower row – entire representative unit

The constraints and interactions between monofilaments and outer layers were also defined. “Tie” constraints were used to connect the monofilaments and outer layers. At step 1, there were no rotation constraints for the “tie”, and all rotation degrees of freedom were free. Hence, a loose structure of the fabric at its initial stage of deformation was simulated. At step 2, the rotation degrees of freedom were fully constrained to describe the fastening effects in the real fabric. “Hard” contacts were defined between monofilaments and outer layers; friction between them was neglected.

The deformed FE model is presented in Figure 10b, which demonstrates that the compression behavior of the spacer fabric is not a simple compression process due to the sandwich structure of the material. Shear stresses and contacts play very important roles in compressive deformation of the material. When the compression displacement is applied, the upper outer layer of the fabric slides, driven by

the shear stress generated by deformed monofilaments. The same phenomenon is also obtained from the results of mCT scanning (Figure 4). And during compression, monofilaments retain their contact to the outer layers. As a result, the effective length of the monofilaments becomes smaller. During the compression, the monofilaments tend to collapse on the internal sides of outer layers. Then, when the shapes of the monofilaments deform due to the changeable constraints, the compression mechanism of the overall fabric becomes more complicated.

Figure 11 shows the top view of the FE model during its compression, which

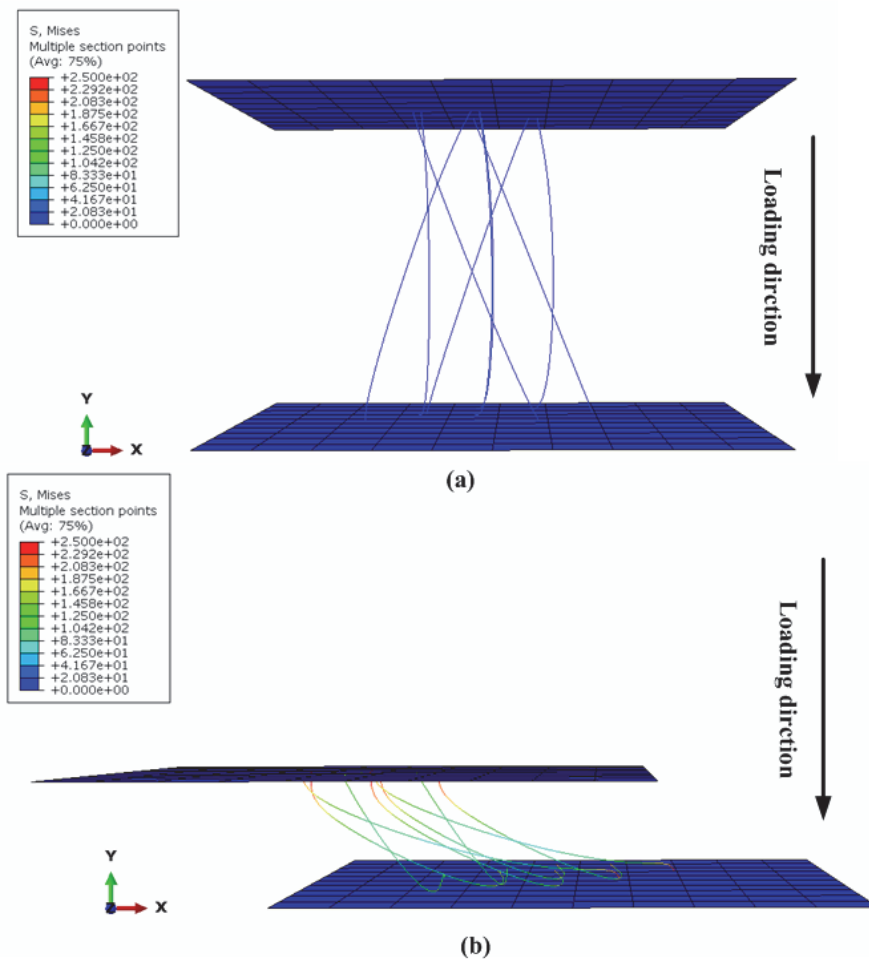


Figure 10: Finite element model of spacer fabric: (a) undeformed model; (b) deformed model

demonstrates the change in the direction of shear stress generated by the deformed monofilaments. At the initial stage of the deformation, the shear stress is caused by the unsymmetrical shape of monofilaments, as shown in Figure 9 (side view). So, the shear stress drives the upper outer layer sidewise along z direction. As the model is deformed further, the upper outer layer slides along both z and $-x$ directions (Figure 11b), while the monofilaments start to collapse. When the monofilaments start to contact the outer layers and slide on their internal surfaces, the direction of the shear stress is oriented along $-x$ and $-z$ directions (Figure 11c, 11d). At the end of the compression, the shear stress is along $-x$ direction only (Figure 11e), linked to pronounced collapse of all the monofilaments.

To compare the simulation results with the experimental data, the force-displacement relationship of the representative unit has to be converted to the one for a specimen with dimensions used in experiment – $100\text{ mm} \times 100\text{ mm}$. According to the density of needles in the knitting machine, the effective area of a representative unit with eight monofilaments is 9.72 mm^2 . Hence, a specimen with area of $100\text{ mm} \times 100\text{ mm}$ includes 1028.7 representative units. Therefore, the respective force F_s on the specimen with $100\text{ mm} \times 100\text{ mm}$ area is:

where F_r is the force acting on the used representative unit.

Figure 12 gives a comparison between the results of the simulation and experimentally obtained force-displacement diagram. At the initial stage, a good agreement is obtained, the force increases slowly, which proves the ends of the monofilament are not constrained at this stage of the deformation. When the model is compressed by a further displacement (stage II), a sharper force increase is obtained than at stage I. The change is due to the additional constraints applied to the ends of monofilaments at this stage of compression. However, a deviation between simulation and experimental results can be observed. When the displacement surpasses 0.8 mm, the increase of the calculated force is slower than that observed in the experiment. The difference is due to the assumption of the FE model that does not account for the effects of contacts and inter-friction between monofilaments. Besides, the intricate structure of the outer layers is reduced to plates, possibly neglecting more complex constraints to the monofilaments. Neglecting the interactions between the outer layers and monofilaments as in real-life specimens can also affect the simulation results. In addition, in the experiments, stage III of the compression is achieved earlier than in numerical simulations due to its faster increase in force at stage II. However, both the calculated and experimental results demonstrate a nearly constant force magnitude at a similar level at this stage. The phenomenon proves that the shear stress is the most important factor affecting the deformation mechanism of the spacer fabric. And the shear stresses are governed by the morphologies of monofilaments and the constraints at their ends.

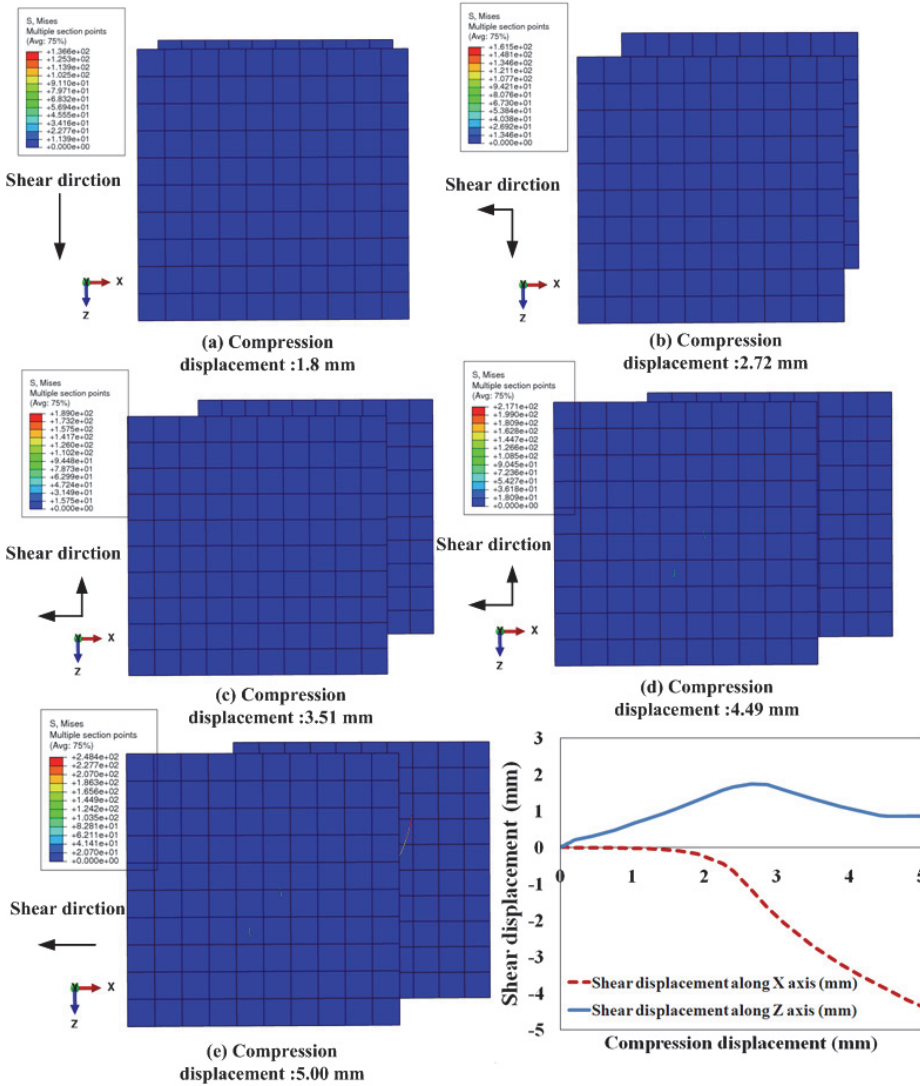


Figure 11: Effects of shear stress on deformation mechanism of spacer fabric

5 Conclusions

Both experimental studies and numerical analysis were used to investigate the compression mechanism of the spacer sandwich fabric. The experimental results show that the compression behavior of the spacer fabric is very complex, determined by compression, shearing, bending, and contacts modes. Four main stages of this pro-

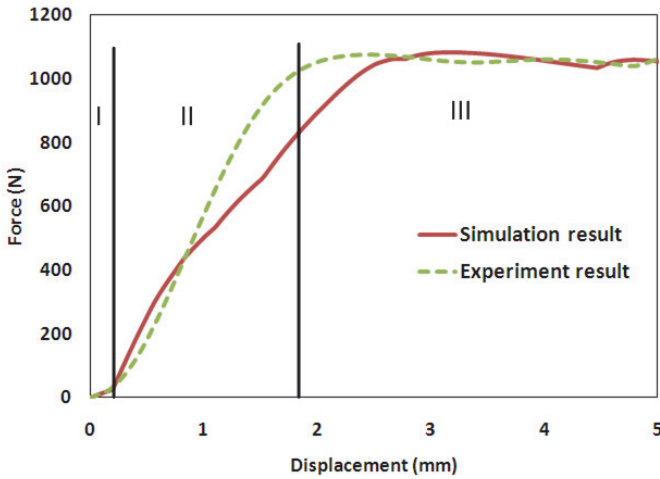


Figure 12: Comparison of force-displacement curves of spacer fabric for experiments and simulations

cess could be defined. Especially, stage III, having a nearly constant force during compression, is of particular interest for some special applications such as protection and energy absorption. The nonlinear mechanical property is defined by the material's structure and the mechanical properties of monofilaments. Therefore, to improve the compression and impact properties of the material, it is important to understand its deformation mechanisms based on the features of its structure.

The results of micro-CT scanning provide 3D images of un-deformed and deformed material, which vividly demonstrate its deformation under different compression displacements. Comparison of mCT data with experimental observations and the results of FE models demonstrate a good agreement.

The finite element method was used to predict the initial shape of compressed monofilaments of three different kinds. The obtained results were used to construct the geometry model of a representative unit of the fabric.

A finite element model was developed to describe the overall compression behavior of the material based on the initial shapes of monofilaments. From the results of the simulation, it is found that the compression mechanism of the spacer fabric is affected by its loose structure, shearing and bending of monofilaments as well as the contacts between monofilaments and outer layers. At the initial stage of the compression, the relatively slow increase in the force is due to the loose structure of the fabric. Then, the structure of the fabric is fastened by further deformation, and

the force of the overall fabric increases rapidly. It is because of the additional constraints to the deformation and rotation of the monofilaments and the effects contributed by the contacts between monofilaments and outer layers. When the fabric achieves even higher compression, the observed constant force is due to the shear of monofilaments. Hence, the developed finite element model provides a powerful tool to study the mechanical properties of the material based on its complicated structure and mechanical properties of its components. Based on the model, it is possible to separately analyze these effective features that would be impossible in real-life experiments, and to obtain a deeper understanding of material's properties of knitted spacer fabrics.

Acknowledgements

The authors would like to acknowledge the funding support from the Hong Kong Polytechnic University (Grant No. 1-ZV0M).

Reference

Armakan, D.; Roye, A. (2009): A study on the compression behavior of spacer fabrics designed for concrete applications, *Fibers and Ploymers*, vol. 10, no. 1, pp. 116-123.

Hou, X.; Acar, M.; Silberschmidt, V. (2009): 2D Finite Element Analysis of Thermally Bonded Nonwoven Materials: Continuous and Discontinuous Models, *Computational Material Science*, vol. 46, no. 3, pp. 700-707.

Hou, X.; Acar, M.; Silberschmidt, V. (2011a): Finite Element Simulation of Low-density Thermally Bonded Nonwoven Materials: Effects of Orientation Distribution Function and Arrangement of Bond Points, *Computational Material Science*, vol. 50, no. 4, pp. 1292-1298.

Hou, X.; Acar, M.; Silberschmidt, V. (2011b): Non-uniformity of Deformation in Low-density Thermally Point Bonded Non-woven Material: Effect of Microstructure, *Journal of Materials Science*, vol. 46, no. 2, pp. 307-315.

Liu, Y.; Hu, H. (2011): Compression Property and Air Permeability of Weft Knitted Spacer Fabrics, *Journal of The Textile Institute*, vol. 102, no.5, pp.366-372.

Miao, X.; Ge, M. (2008): The Compression Behavior of Warp Knitted Spacer Fabric, *Fibres & Textile in Eastern Europe*, vol. 16, no. 1(66), pp. 90-92.

Sheikhzadeh, M.; Ghane, M.; Eslamian, Z.; Pirzadeh, E. (2010): A Modeling Study on the Lateral Compressive Behavior of Spacer Fabrics, *The Journal of The Textile Institute*, vol. 101, no. 9, pp. 795-800.

Skock-Hartmann, B.; Diestel, Q.; Bovenkert, J.; Cherif, C.; Gries, T.; Eckstein, L. (2009): The Development of Integral Bonnet Systems Based on Innova-

tive 3D Textile Structures for Protecting Pedestrians, *Kettenwirk Praxis*, vol. 4, pp. 20-22.

Vassiliadis, S.; Kallivretaki, A.; Psilla, N.; Provatidis, C.; Mecit, d.; Roye, A. (2009): Numerical Modeling of the Compressional Behavior of Warp-knitted Spacer Fabrics, *Fibres&Textile in Eastern Europe*, vol. 17, no. 5 (76), pp. 56-61.

Wyk, V. (1946): Note on the Compressibility of Wool, *Journal of The Textile Institute*, vol. 37, pp. 285.

Ye, X.; Hu, H.; Feng, X. (2008): Development of the Warp Knitted Spacer Fabrics for Cushion Applications, *Journal of Industrial Textiles*, vol. 3, pp. 213-223.

Ye, X.; Hu, H.; Araujo, M. (2007): Application of Warp-Knitted Spacer Fabrics in Car Seats, *The Journal of The Textile Institute*, vol. 4, pp. 337-340.

Yip, J.; Ng, S. (2008): Study of Three-dimensional Spacer Fabrics: Physical and Mechanical Properties, *Journal of Materials Processing Technology*, vol. 206, no. 1-3, pp. 359-364.